Civil Engineering Dimension, Vol. 25, No. 2, September 2023, 126–134
ISSN 1410-9530 print / ISSN 1979-570X online
DOI: https://doi.org/10.9744/CED.25.2.126-134

Evaluation of ASTM D 1143/D 1143M-07 and Chinese Code JGJ 106-2014 for Pile Load Testing using Finite Element Method

Lim, A.[1]* and Sukiwan, O.A.[1]

Abstract: Pile foundation is a structural element utilized to transmit structural load into the soil mass. During design processes, many empirical equations used to estimate axial pile capacity, and a pile load test is conducted to validate the design. In Indonesia, it is common to adopt ASTM D 1143/D 1143M-07 for pile testing. Chinese Code JGJ 106-2014 is another viable option, which has gained popularity recently. This study investigated the load–settlement curves obtained using both codes. The analyses were simulated using the Mohr–Coulomb and the Hardening Soil models. The Hardening Soil model yielded more reasonable load–settlement and load–excess pore water pressure curves than the Mohr–Coulomb model. The reason due to the Mohr–Coulomb model unable to capture the non-linear behavior of soil properly. Furthermore, the results showed that ASTM D 1143/D 1143M-07 and JGJ 106-2014 yielded comparable results. Hence, both methods could be substituted each other.

Keywords: ASTM D 1143/D 1143M-07; Chinese Code JGJ 106-2014; Finite Element Method; Load–settlement curve; Static loading test.

Introduction

Static load testing is commonly used to determine pile performance. Through the test, an engineer could evaluate the axial pile capacity as well as pile settlement. Conducting this test should abide by a standardized code. For example, ASTM D 1143/D 1143M-07 (standard test methods for deep foundations under static axial compressive load) [1] and Chinese Code JGJ 106-2014 (technical code for testing of building foundation piles) [2].

ASTM D 1143/D 1143M-07 [1] and Chinese Code JGJ 106-2014 [2] demonstrate five differences, as listed in Table 1: the maximum applied load, load increments and decrements, as well as the time intervals between load increments and decrements. Thus, the obtained load–settlement curves are arguably different. In this work, the results obtained from ASTM D 1143/D 1143 M-07, especially Procedure B (maintained test) and Procedure G (cyclic loading test), and Chinese Code JGJ 106-2014 (vertical compression static loading test for single pile) were compared.

Teshager [3] conducted finite element analysis for static pile load testing using both axisymmetric and three-dimensional (3D) analyses and compared the results obtained by two models, the linear-elastic model for piles and the Mohr–Coulomb (MC) model for soils.

[1,2] Department of Civil Engineering, Parahyangan Catholic University, Jln. Ciumbuleuit No. 94, Bandung 40141, INDONESIA

*Corresponding author; Email: aswinlim@unpar.ac.id

Note: Discussion is expected before November, 1st 2023, and will be published in the "Civil Engineering Dimension", volume 26, number 1, March 2024.

Received 06 April 2023; revised 25 August 2023; accepted 01 September 2023.

The parameters for numerical modeling were estimated using correlations based on the Standard Penetration Test values of soil as well as unconfined compressive strength of rock core samples. It also included a mesh convergence study in which one of the models was selected, and the effect of mesh size was studied. The sizes used were described as very coarse, coarse, medium, fine, and very fine. Very fine mesh size provided better accuracy compared to the field test. Krasinski and Wiszniewski [4] used a field load test on an instrumented pile and compared them with numerical simulation under similar conditions. Hardening soil model was adopted [5] and it concluded that both the field data and numerical analysis contain errors and inaccuracies, such as incorrect contact interface modeling leading to misleading skin friction values, overly simplified soil model parameters, pile imperfections, and residual loads in the pile load test procedure. Moreover, Yi [6] (2004) reported that the finite element method (FEM) could yield reasonable pile load testing results in terms of load transfer and load–settlement curves.

Furthermore, Yang and Liu [7] as well as Abdel-Azim et al. [8] showed that 3D finite element analysis may produce agreeable results when compared with field tests. Yang and Liu [7] modeled a prestressed concrete pipe pile–composite foundation, while Abdel-Azim et al. [8] modeled a piled raft foundation, indicating that finite element analysis could be applied to various cases. Another finite element modeling software, ABAQUS, which was used by Haouari and Bouafia [9] as well as Knappett and Madabhushi [10], was shown to produce reliable results. According to Haouari and Bouafia [9], the results obtained using ABAQUS were coherent with the experimental results. In addition, Knappett and Madabhushi [10] showed that

Table 1. The Testing Procedure of ASTM D1143/D1143M-07 and JGJ 106-2014

Differences	ASTM D 1143 / D 1143M-07		JGJ 106-2014
	Procedure B (Maintained Test)	Procedure G (Cyclic Loading Test)	Vertical Compression Static Loading Test Single Pile
Load increment	25% design load	25% design load [a]	10% design load
Maximum load	200% design load	150% design load [b]	100% design load
Loading interval (s)	5400 to 7200	3600 or 1200 [c]	5400
Load decrement	25% maximum load	equal to load increment	20% design load
Unloading interval (s)	3600	1200	3600

Note:
Design load is the load that the pile is expected to carry
[a] when reapplying the load to each preceding load level, it is 50% of the design load.
[b] 150% is the maximum load, but unloading occurs when 50% and 100% of design load are reached.
[c] 3600 s (60 min) is the initial loading interval whereas 1200 s (20 min) is used when reapplying load.

ABAQUS presented acceptable predictions, validated using six pile group models.

FEM has been well developed for pile load testing simulations. However, the results obtained from various pile testing procedures have not been compared to date. Considering the high cost of conducting a static pile load test using different procedures, numerical analyses were applied to obtain the study objective. In this study, a homogeneous clay and two types of soil constitutive models, the MC model and the hardening soil (HS) model [5], were adopted. Later, the load–displacement curves and the load–excess pore pressure curves obtained from three different pile loading procedures were discussed. Finally, a well-documented pile load test was modeled to verify the analysis results. Finally, the conclusions were summarized based on the analysis results.

Research Methodology

The research methodology consists of two parts. In Part 1, homogeneous clay soil was chosen to simulate the three procedures, as listed in Table 1. The purpose of these simulations was to observe and investigate each procedure in idealized soil conditions. In addition, mesh convergence was conducted in Part 1 for comparison with the results of the simulations. In Part 2, a well-documented pile load test located in North Jakarta was simulated to validate the findings obtained in Part 1 with real soil stratification. Then, the conclusions were drawn from the obtained results. All analyses were performed using a commercial software, namely PLAXIS 2D V20.

Numerical Modeling

Two-dimensional (2D) finite element analyses were conducted using PLAXIS 2D V20. Figure 1 shows the finite element mesh used to conduct the analyses. The pile length (L) and diameter (D) used in the model were 10 m and 1 m, respectively. Due to symmetry, only half of the geometry was modeled. Moreover, fifteen-node triangular elements were used to simulate the soil cluster, and the very fine mesh was selected in this model. In total, 2577 elements were generated in the model. The groundwater table was also modeled and located at the ground surface. The vertical boundary of the model was 20 m, which was double the length of the pile and thus did not influence the stress distribution that reaches the pile base.

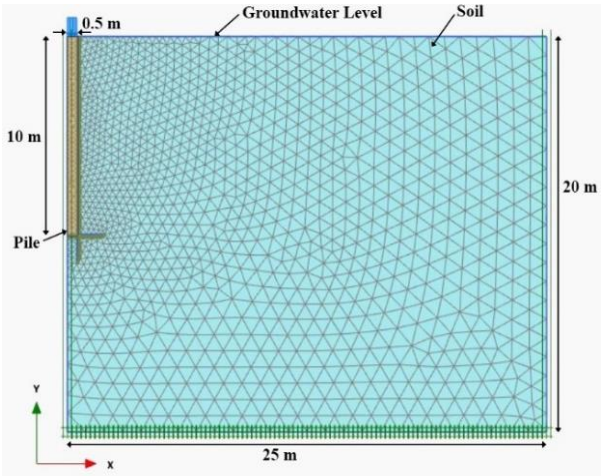

Figure 1. Finite Element Model for Analysis

Teshager [3] observed that pile settlement results were affected when analyses were performed with closer limits. The interface was extended beyond the end of the structure to avoid locking and inaccurate stress results at the tip or corners [11]. Thus, the bottom boundary was set to the fixed boundary, and the side boundaries were set to the roller boundary.

The MC and HS models were adopted to simulate the soil behavior under the undrained analysis for the fine-grain soil. The MC model is a well-known linear-elastic perfectly plastic model, which can be used for the initial approximation of soil behavior. This model requires a total of five parameters: modulus of elasticity (E), Poisson ratio (υ), cohesion (c), friction angle (ϕ), and dilatancy angle (ψ). Even though the model can lead to increased stiffness with depth, it does not include stress dependency or stress path dependency for stiffness. In contrast, the HS model is

a hyperbolic model with a nonlinear stress–strain relationship and stress dependency of stiffness moduli. To more accurately describe soil stiffness, this model uses secant stiffness in standard drained triaxial testing (E_{50}^{ref}), tangent stiffness for primary oedometer loading (E_{oed}^{ref}), unloading/reloading stiffness (E_{ur}^{ref}), and power for the stress-level dependency of stiffness (m). It also utilizes the same failure parameters as the MC model, which include cohesion (c), friction angle (ϕ), and dilatancy angle (ψ). Meanwhile, the structural element was assumed to behave as linear-elastic. Those two soil models are well-known for geotechnical analyses and yield reasonable results [12-14].

Input Parameters

Homogenous clay soil with an N_{SPT} of 6 was used in this analysis of Part 1. According to Terzaghi and Peck [15], clay soil with N_{SPT} = 6 has a range of undrained shear strength (S_u) in the range of 25–50 kPa. In this analysis, S_u of 30 kPa was chosen. Moreover, the undrained Young modulus (E) was obtained from correlation, proposed by Jamiolkowski et al. [16], where E_u/S_u = 100–300. In this case, E_u/S_u = 150 was selected. Then, using elasticity theory, the drained Young modulus was obtained, which was about 80% of E_u. Other parameters followed typical values for soft-to-medium clay [17-19]. In addition, for simplicity, the coefficient of permeability was the same in both directions ($k_x = k_y$). The input parameters for the MC and HS models are listed in Tables 2 and 3, respectively. $E_{oed}^{ref} = E_{50}^{ref}$ and $E_{ur}^{ref} = 3\,E_{50}^{ref}$ based on the PLAXIS manual.

Table 2. Input Parameters for Mohr-Coulomb Model

Soil type	γ (kN/m³)	γsat (kN/m³)	c (kPa)	ϕ (°)	E (kPa)	kx=ky (m/s)	υ
Clay	16	17	30	0	3600	10^{-10}	0.3

The pile used in the model was concrete with a modulus of approximately 21 GPa and a Poisson ratio of 0.15. In the analyses, the interface friction (R_{inter}) between the structural elements and adjacent soils was set as rigid (R_{inter} = 1).

The ultimate load (Q_u) was estimated to be the sum of the pile point bearing capacity (Q_p) and its frictional resistance (Q_s) [20], calculated using the following equations:

$$Q_s = \sum p\ \Delta L\ f_s \quad (1)$$

where p is the perimeter of the pile section, ΔL is the incremental pile length, and f_s is the unit friction resistance (p and f_s are constant). Q_p and f_s are estimated according to Meyerhof [21], and Tomlinson & Woodward [22].

$$Q_p = 9\ Su\ A_p \quad (2)$$

$$Q_p = 9 \times 30 \times \frac{\pi}{4} \times 1^2 = 212.06\ kN : f_s = \alpha\ c_u \quad (3)$$

$$Q_s = \pi \times 1 \times 10 \times 1 \times 30 = 942.48\ kN$$

where S_u is the undrained shear strength of soil below the pile tip, A_p is the area of the pile tip, and α is the adhesion factor.

Hence, the ultimate load was 1154.54 kN. For the design load (Q), the ultimate load was divided by a safety factor value. The value of safety factor was 3. Therefore, the design load was 384.85 kN. Again, the design load is the load that the pile is expected to carry.

As mentioned earlier in Table 1, the maximum load of each procedure is different. The maximum loads of Procedure B, Procedure G, and Chinese Code JGJ 106-2014 vertical compression static loading test for a single pile were 200%, 150%, and 100% of the design load, respectively.

For comparison purposes, the same maximum load was applied in each procedure. In such a condition, the design load of each procedure was adjusted. Because Procedure B claimed 200% of the design load as the maximum load, the calculated design load (384.85 kN) was applied to Procedure B. For Procedure G and JGJ 106-2014, the design load was adjusted linearly, as listed in Table 4.

Table 4. The Design Load used for Analyses.

Procedure	Maximum Load (kN)
ASTM D 1143/D 1143M-07 Procedure B	200% of 384.8
ASTM D 1143/D 1143M-07 Procedure G	150% of 513.1
JGJ 106-2014	100% of 769.7

Modeling Procedure

The numerical modeling stages consisted of pile installation and load testing. As mentioned before, the load test for each procedure had different loading and unloading increments, as well as different time intervals for loading and unloading. In this analysis, a time-coupled analysis was selected. In PLAXIS 2D V20, the consolidation-type analysis was used.

Table 3. Input Parameters for Hardening Soil Model

Soil type	γ (kN/m³)	γsat (kN/m³)	c (kPa)	ϕ (°)	E_{50}^{ref} (kPa)	E_{oed}^{ref} (kPa)	E_{ur}^{ref} (kPa)	kx=ky (m/s)	υ	m
Clay	16	17	30	0	3600	3600	10800	10^{-10}	0.3	1

Table 5 lists the modeling procedure of Procedure B. For Procedure B, the load applied to the pile head increased every 5400 s (90 min) for 25% of the design load until the value reached 200% of the design load. Then, 25% of the maximum load, which is 50% of the design load if it reaches 200% of the design load, was removed every 3600 s (60 min).

Table 5. Stage Construction of ASTM D 1143/D 1143M-07 Procedure B Simulation

Stage	Activity	Stage	Activity
0	Initial condition	8	Loading 150% for 5400 s
1	Activate pile	9	Loading 175% for 5400 s
2	Loading 0%	10	Loading 200% for 5400 s
3	Loading 25% for 5400 s	11	Unloading 150% for 3600 s
4	Loading 50% for 5400 s	12	Unloading 100% for 3600 s
5	Loading 75% for 5400 s	13	Unloading 50% for 3600 s
6	Loading 100% for 5400 s	14	Unloading 25% for 3600 s
7	Loading 125% for 5400 s	15	Unloading 0%

Table 6 lists the modeling procedure of Procedure G. Procedure G is a cyclic loading test with 3 cycles for a single pile that has a maximum load of 50%, 100%, and 150% before unloading occurs. For the first cycle, the load was applied every 3600 s (1 h) with an increment of 25% of the design load until it reaches 50% of the design load. Then, every 1200 s (20 min), the load was removed in decrements equal to the loading increments. After removing the maximum applied load, the load was reapplied to each preceding level with increments of 50% of the design load, allowing 1200 s (20 min) between increments. Hence, the second cycle's first load was 50% of the design load and increased by 25% every 3600 s (1 h) until 100% of the design load was reached. The last cycle's first load was 50% of the design load, continued with 100% of the design load; afterward, the load was increased by increments of 25% of the design load until 150% of the design load was achieved.

Table 6. Stage Construction of ASTM D 1143/D 1143M-07 Procedure G Simulation

Stage	Activity	Stage	Activity
0	Initial condition	11	Unloading 50% for 1200 s
1	Activate pile	12	Unloading 0% for 1200 s
2	Loading 0%	13	Loading 50% for 1200 s
3	Loading 25% for 3600 s	14	Loading 100% for 1200 s
4	Loading 50% for 3600 s	15	Loading 125% for 3600 s
5	Unloading 25% for 1200 s	16	Loading 150% for 3600 s
6	Unloading 0% for 1200 s	17	Unloading 125% for 1200 s
7	Loading 50% for 1200 s	18	Unloading 100% for 1200 s
8	Loading 75% for 3600 s	19	Unloading 50% for 1200 s
9	Loading 100% for 3600 s	20	Unloading 0%
10	Unloading 75% for 1200 s		

Table 7 lists the modeling procedure of JGJ 106-2014 with a step load of $^1/_{10}$ or 10% of the maximum load, and the unload was taken as twice the step load, which was 20% of the maximum load. Similar to that in Procedure B, the step load was increased every 5400 s (90 min) while unloading was performed every 3600 s (1 h).

Table 7. Stage Construction of JGJ 106-2014 Simulation

Stage	Activity	Stage	Activity
0	Initial condition	9	Loading 70% for 5400 s
1	Activate pile	10	Loading 80% for 5400 s
2	Loading 0%	11	Loading 90% for 5400 s
3	Loading 10% for 5400 s	12	Loading 100% for 5400 s
4	Loading 20% for 5400 s	13	Unloading 80% for 3600 s
5	Loading 30% for 5400 s	14	Unloading 60% for 3600 s
6	Loading 40% for 5400 s	15	Unloading 40% for 3600 s
7	Loading 50% for 5400 s	16	Unloading 20% for 3600 s
8	Loading 60% for 5400 s	17	Unloading 0%

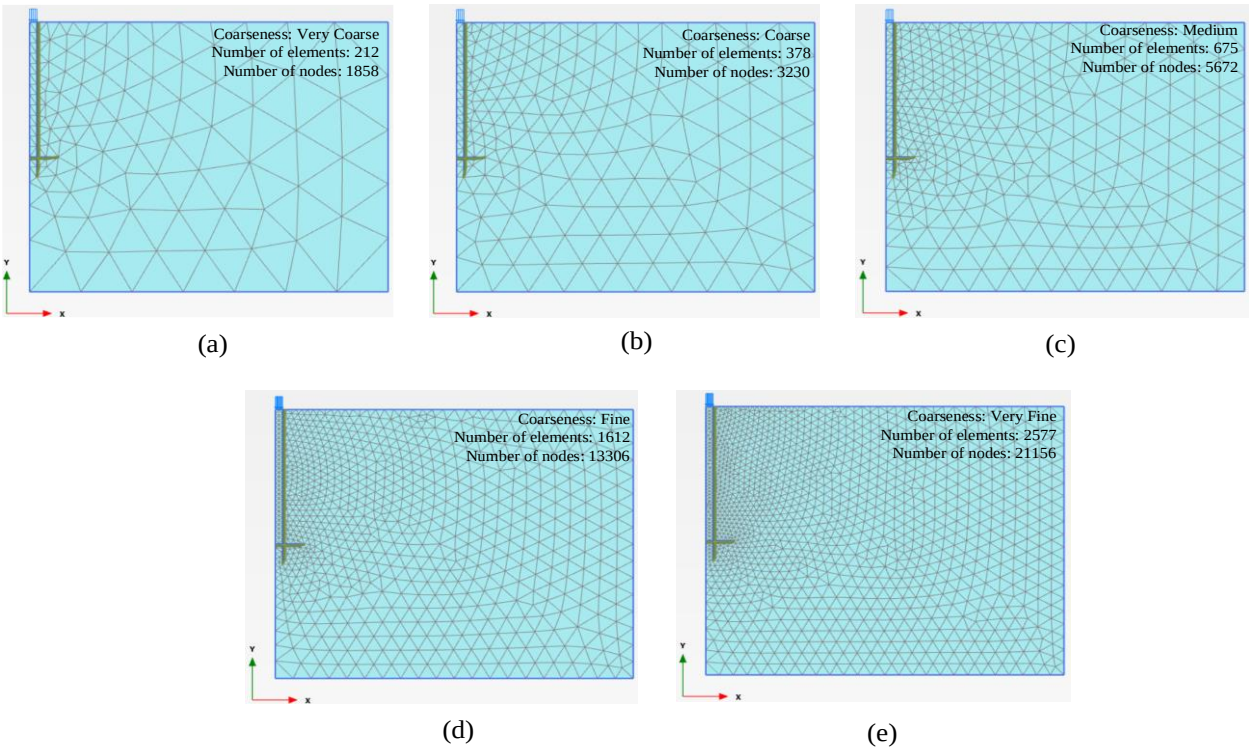

Figure 2. The Variation of Mesh Coarseness for Mesh Convergence Analysis

Results

Part One: Homogenous Clay Soil

Prior to the simulation of all procedures, a model was chosen to study the mesh convergence analysis. In total, 5 variations of mesh coarseness were modeled, as depicted in Figure 2. The mesh coarseness was varied from the very coarse to very fine mesh with 212 to 2577 elements, respectively.

The load–settlement curves of different mesh coarseness are shown in Figure 3. The fine mesh and the very fine mesh demonstrated comparable results, which almost converged. Hence, in this study, the very fine mesh was chosen to model all the analyses.

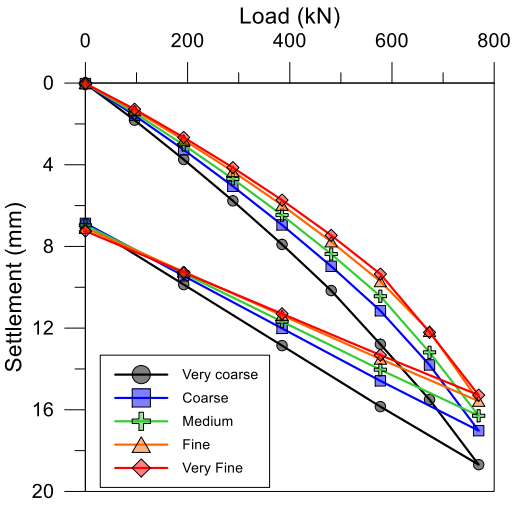

Figure 3. The Load-settlement Curve of Different Mesh Coarseness

Figure 4 shows the load–settlement curves obtained using three different procedures for clay soil. Similar load–settlement curves were obtained using either the MC model or the HS model. Thus, the differences between the three procedures were negligible.

However, the load–settlement curves obtained by the MC model and the HS model were different, as shown in Figure 5.

The MC model showed a linear load–settlement curve, while the HS model yielded a nonlinear load–settlement curve. At the final load, the difference in the calculated settlement was about 11 mm. These results show that the MC model adopts a linear-elastic behavior when the soil is in an elastic state, while the HS model adopts a nonlinear behavior (hardening rule) when the soil is in an elastic state. Hence, both results are reasonable, depending on the soil model used for analysis. Because soil behaves nonlinearly, the result of the HS model is more reliable than the MC model.

Figure 6 shows the load–excess pore water pressure curves for different models within the same procedure. A similar trend was also observed where the MC model generated linear excess pore pressure when the load increased. When the load was unloaded to zero, both the MC and HS models had excess pore pressure, which was yet to be dissipated. Although load–excess pore pressure curves are seldom investigated in the field test due to the lack of instrumentation, this result indicates that the shear stress of soil might decrease during a pile load test. Hence, the obtained

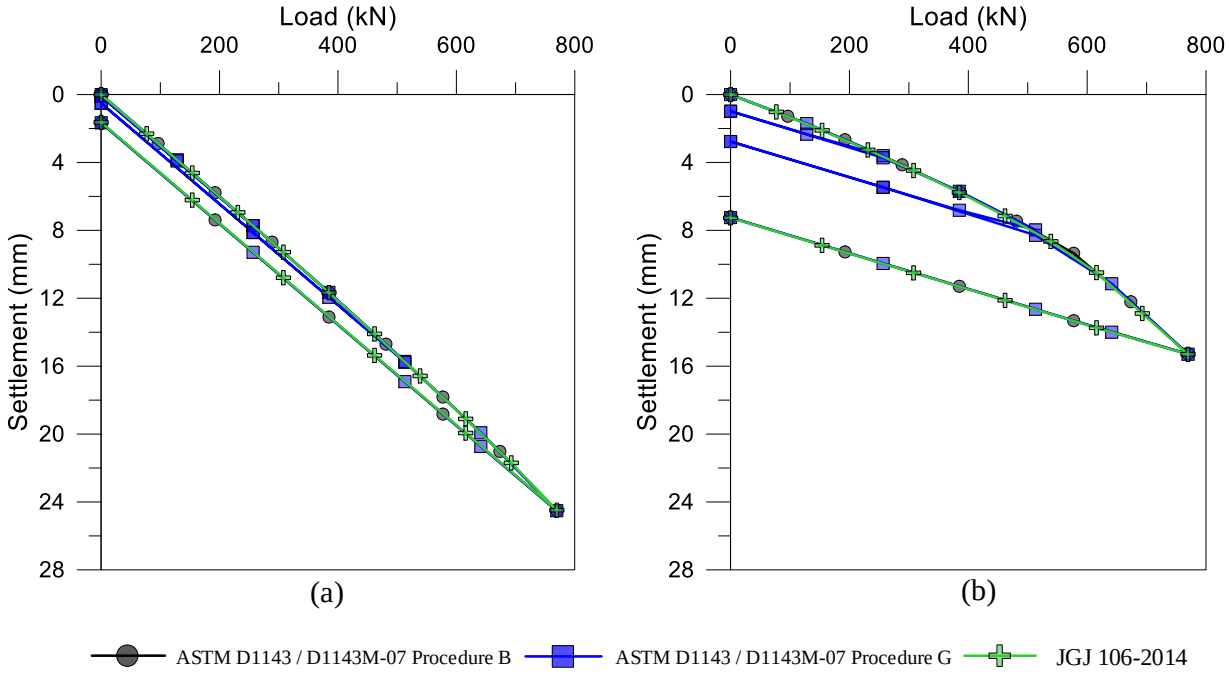

Figure 4. Load-Settlement Curve obtained from Three Different Procedures using (a) MC Model, (b) HS Model for Clay Soil

load–settlement curve might be conservative from the real performance of the pile. From the design point of view, this behavior is acceptable.

In addition, a parametric study was conducted to study the effect of the interface strength, as shown in Figure 7. Three variations of the interface strength,

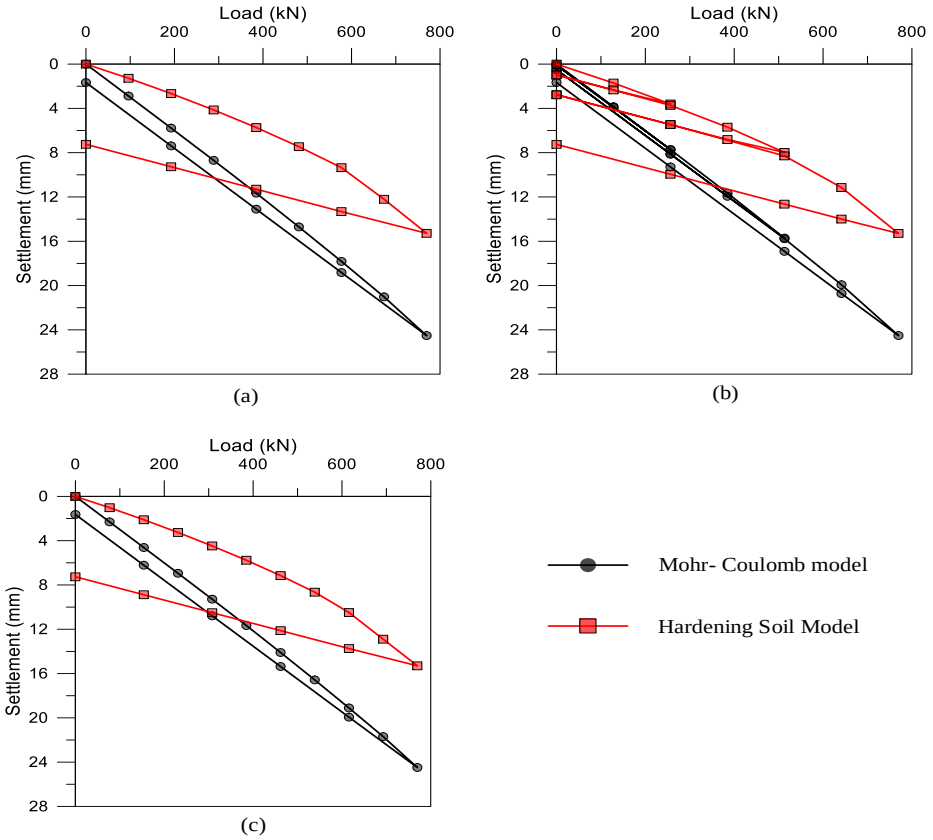

Figure 5. Load-Settlement Curve of (a) Procedure B, (b) Procedure G, (c) JGJ 106-2014

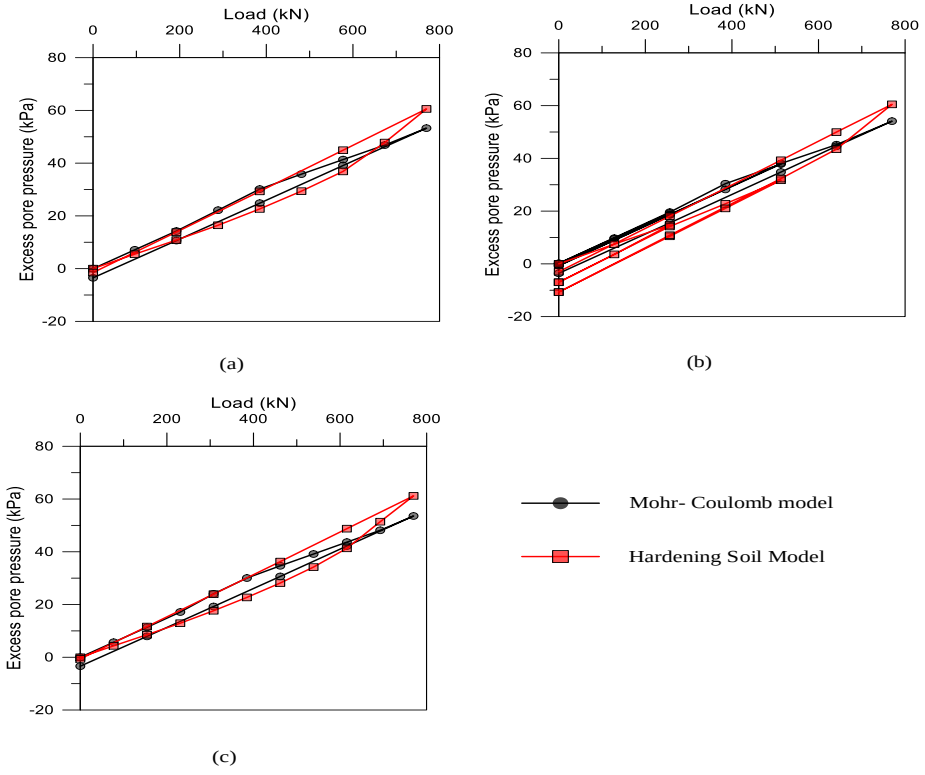

Fig. 6. Load-Excess Pore Water Pressure Curve of (a) Procedure B, (b) Procedure G, (c) JGJ 106-2014

R_{inter} = 1.0, R_{inter} = 0.9, and R_{inter} = 0.8, were applied using Procedure B. The decrease in R_{inter} yielded a larger settlement to reach a similar load, especially for the load exceeding 500 kN. A similar trend was also reported by Lim et al. 2022. In this study, R_{inter} was equal to 1 following the default value in PLAXIS. Although the quantitative values showed slight variations, the trends of the load–settlement curves were similar. Hence, the different assignment of R_{inter} does not affect the drawn conclusions.

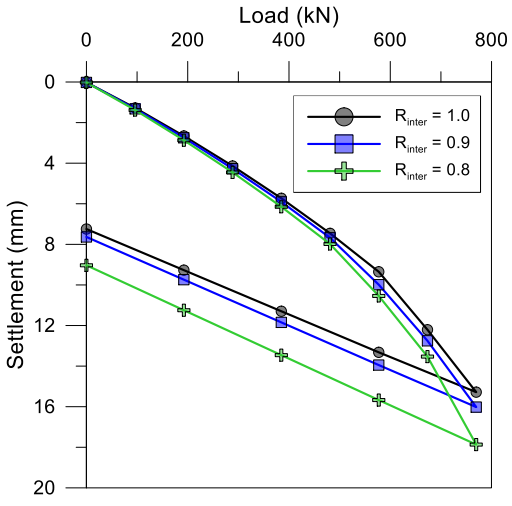

Figure 7. The Load-settlement Curve of Different R_{inter} Values

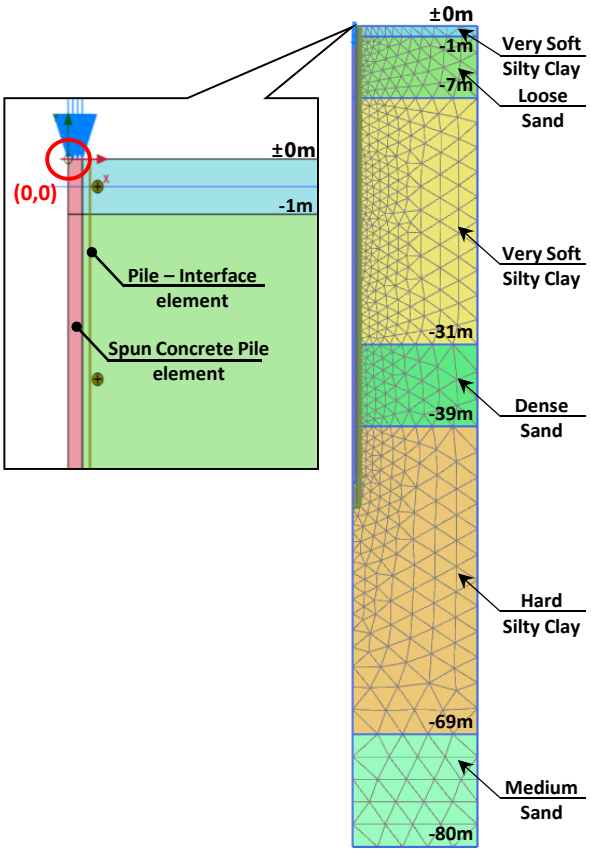

Figure 8. Finite Element Model for the Case History [23]

Part Two: A Well-documented Pile Load Test

A well-documented pile load test was used to validate the findings obtained in Part 1. The pile load test was tested using Procedure B but without the unloading scheme. The project was located in North Jakarta, Indonesia. Figure 8 depicts the FEM for analysis [23]. The pile diameter was 600 mm, and the pile length was 44.5 m. The soil was predominant with very soft silt clay, which takes place from 7 to 31 m below the ground level.

For this purpose, a back analysis was executed to determine E_{50}^{ref}, E_{oed}^{ref}, and E_{ur}^{ref}. A study by Saptyanto [24] found a correlation between E_{50}^{ref} and $N_{1(60)}$ for both fine-grained and coarse-grained soils. On average, E_{50}^{ref} (MPa) = 1.3 $N_{1(60)}$ and E_{50}^{ref} (MPa) = 2 $N_{1(60)}$ with a maximum of E_{50}^{ref} (MPa) = 4 $N_{1(60)}$ and E_{50}^{ref} (MPa) = 7.5 $N_{1(60)}$ for fine-grained and coarse-grained soils, respectively. Hence, the N_{SPT} data from the project were converted to N_{60} and $N_{1(60)}$ using correlations reported by Rahardjo [25] and Liao and Whitman [26], respectively.

$$N_{60} = \eta \times N_{SPT} \quad (4)$$

$$N_{1(60)} = N_{60} \times \sqrt{\frac{100\ kPa}{\sigma'_v}} \quad (5)$$

where N_{SPT} is Standard Penetration Test (SPT) blow count per 300 mm, N_{60} is corrected value of N_{SPT} against standard efficiency, $N_{1(60)}$ is corrected value of N_{SPT} against standard efficiency and effective vertical overburden pressure, η is the correction factor for efficiency, and σ'_v is the effective vertical overburden pressure.

The efficiency used for Equation (4) was 80%, as suggested by Rahardjo [25] for an automatic trip hammer. The effective vertical overburden pressure was calculated in the middle of each layer. Table 8 summarizes the soil stratifications as well as input parameters used for the FEM. Moreover, the groundwater table was located 0.5 m below the ground level.

In Table 9, E_{oed}^{ref} and E_{ur}^{ref} are equal to E_{50}^{ref} and 3 E_{50}^{ref}, respectively. The pile used for this study was classified as class A1 concrete with a modulus of approximately 30 GPa and a Poisson ratio of 0.2. In the analyses, the interface friction (R_{inter}) between the structural elements and adjacent soils was set as rigid (R_{inter} = 1), as suggested by Lim et al. [23].

In the analyses, the pile was loaded with a maximum load of 3500 kN using three different procedures. Then, the obtained results were compared with the

Table 8. Input Parameter for Case-history of Pile Load Testing Project [22]

Layer	Depth (m)	Soil type	N_{SPT}	ϕ (°)	γ (kN/m³)	γ_{sat} (kN/m³)	c (kPa)	υ
1	0.0 – 1.0	very soft – silty clay	2	0	16	17	11	0.35
2	1.0 – 7.0	loose – sand	8	30	16	18	0	0.25
3	7.0 – 31.0	very soft – silty clay	2	0	16	17	11	0.35
4	31.0 – 39.0	dense – sand	32	37	19	21	0	0.3
5	39.0 – 69.0	hard – silty clay	26	0	18	20	156	0.3
6	69.0 – 80.0	medium – sand	27	36	19	21	0	0.3

Table 9. Calculated N_{60}, $N_{1(60)}$, E_{50}^{ref}, E_{oed}^{ref}, and E_{ur}^{ref}

Depth (m)	N_{SPT}	N_{60}	σ'v (kPa)	$(N_1)_{60}$	E_{50}^{ref} (kPa)	E_{oed}^{ref} (kPa)	E_{ur}^{ref} (kPa)
0.5	2	1.6	8.0	5.657	7354	7354	22062
4	8	6.4	35.5	10.742	21483	21483	64449
19	2	1.6	143.5	1.336	1736	1736	5208
35	32	25.6	271.5	15.537	31073	31073	93219
54	26	20.8	465.5	9.641	14461	14461	43383
74.5	27	21.6	676.0	8.308	24923	24923	74769

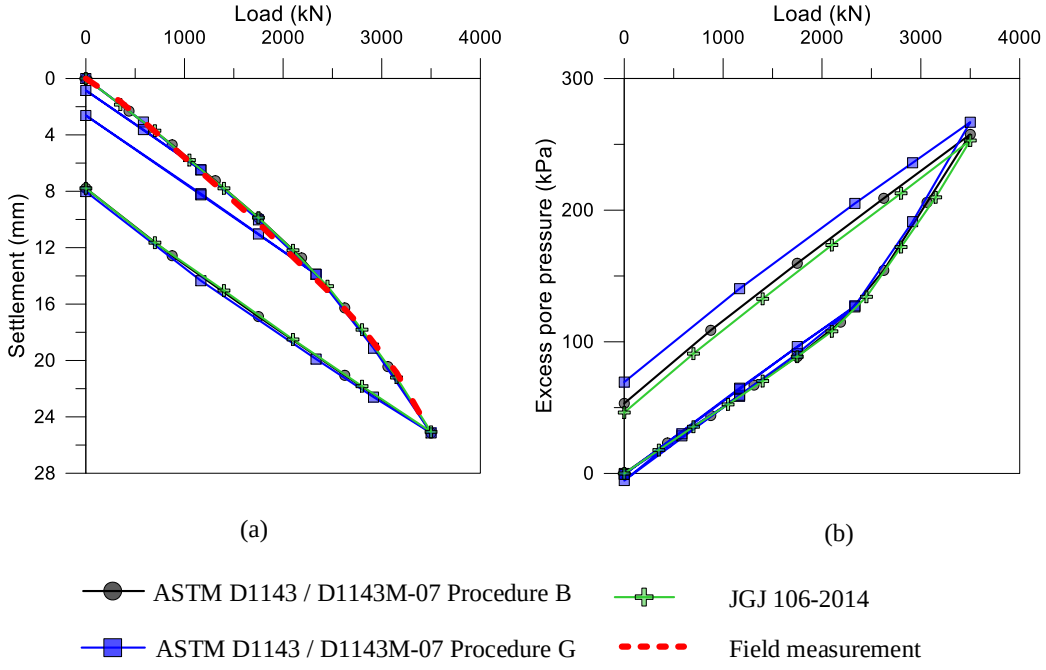

Figure 9. The Results of (a) Load-settlement Curve, (b) Load-Excess Pore Water Pressure for the Case History

field test measurements. As shown in Figure 9a, the load–settlement curves obtained from the analyses yielded a comparable result with the field data, indicating that the FEM model is valid and that the three procedures can substitute for each other. Slight differences (<6%) were obtained for the excess pore water pressure results (Figure 9b) between the three procedures.

Conclusions

Three pile load testing methods, namely ASTM D 1143/D 1143M-07 Procedure B, ASTM D 1143/D 1143M-07 Procedure G, and JGJ 106-2014, were demonstrated. Major findings can be summarized as follows: (1) Different procedures gave approximately the identical settlement and excess pore water pressure values using homogenous clay soil. In addition, the load–settlement curves were identical to each other. The reason due to the loading time for each loading stages were not significantly affecting the pile settlement. Hence, ASTM D 1143/D 1143M-07 Procedure B, ASTM D 1143/D 1143M-07 Procedure G, and JGJ 106-2014 can be used to substitute each other; (2) The HS model yielded more reasonable load–settlement and load–excess pore water pressure curves than the MC model. The reason due to the MC model unable to capture the non-linear behavior of soil properly; (3) A well-documented pile load test verified the conclusions drawn from homogenous clay.

It indicates that the drawn conclusions could be applied for stratified soil layers which is predominant with clays soil as well.

Data Availability Statement

Some or all data, models, or code that support the findings of this study are available from the corresponding author upon reasonable request.

References

1. ASTM D 1143/D 1143M-07, *Standard Test Methods for Deep Foundations Under Static Axial Compressive Load*, ASTM International, 2007.
2. JGJ 106-2014, *Technical Code for Testing of Building Foundation Piles*. Ministry of Housing and Urban-Rural Development of the People's Republic of China, 2014.
3. Teshager, D.K., Numerical Simulation of Static Pile Load Test on Stratified Soil Deposits, *Global Scientific Journal*, 7(11), 2019, pp. 1180–1211.
4. Krasiński, A. and Wiszniewski, M., Static Load Test on Instrumented Pile-Field Data and Numerical Simulations. *Studia Geotechnica et Mechanica*, 39(3), 2017, pp. 17–25. https://doi.org/10.1515/sgem-2017-0026
5. Schanz, T., Vermeer, P.A., and Bonnier, P.G., The hardening-soil model: Formulation and verification., In *Proceedings of The International Symposium Beyond 2000 in Computational Geotechnics*, Amsterdam, The Netherlands, March 18-20, 1999, pp. 281–290. https://doi.org/10.1201/9781315138206-27
6. Yi, L. *Finite Element Study on Static Pile Load Testing*, Master's Thesis, National University of Singapore, 2004.
7. Yang, M. and Liu, S., Field Tests and Finite Element Modeling of a Prestressed Concrete Pipe Pile-Composite Foundatio, *KCSE Journal of Civil Engineering*, 19(7), 2015, pp. 2067–2074. https://doi.org/10.1007/S12205-015-0549-Z
8. Abdel-Azim, O.A., Abdel-Rahman, K., and El-Mossallamy, Y.M., Numerical Investigation of Optimized Piled Raft Foundation for High-Rise Building in Germany, *Innovative Infrastructure Solutions*, Springer, 5(1), 2020. https://doi.org/10.1007/s41062-019-0258-4
9. Haouari, H. and Bouafia, A.A., Centrifuge Modelling and Finite Element Analysis of Laterally Loaded Single Piles in Sand with Focus on P–Y Curves, *Periodica Polytechnica Civil Engineering*, 64(4), 2020, pp. 1064–1074. https://doi.org/10.3311/PPci.14472
10. Knappett, J.A. and Madabhushi, S.P.G., Modelling of Liquefaction-induced Instability in Pile Groups, In *Seismic Performance and Simulation of Pile Foundations in Liquefied and Laterally Spreading Ground (Geotechnical Special Publication (GSP) No. 145) (eds. R. W. Boulanger and K. Tokimatsu),* ASCE, 2005, pp. 225–267. https://doi.org/10.1061/40822(184)21
11. Brinkgreve, R.B.J. and Witasse, R.P.B., Risques associés à l'utilisation de la méthode des éléments finis pour la géotechnique, *Revue Française de Géotechnique,* 140–141, 2012, pp. 11–19. https://doi.org/10.1051/geotech/2012140011
12. Lim, A. and Ou, C.Y., Stress Paths in Deep Excavations under Undrained Conditions and its Influence on Deformation Analysis, *Tunnelling and Underground Space Technology*, 63, 2017, pp. 118-132
13. Lim, A., Ou, C.Y., and Hsieh, P.G., Evaluation of Clay Constitutive Models for Analysis of Deep Excavation Under Undrained Conditions, *Journal of GeoEngineering*, 5(1), 2010, pp. 9-20
14. Lyman, R.A., Lim, A., Rahardjo, P.P., Estimating System Stiffness of Soil Nailing Wall for Deep Excavation in Clay, *International Journal of Civil Engineering*, Springer International Publishing, 20(9), 2022, pp. 1009-1025
15. Terzaghi, K. and Peck, R.B, *Soil Mechanics in Engineering Practice, Second Edition*. John Wiley & Sons, Inc, 1967.
16. Jamiolkowski, M., Lancellotta, R., Pasqualini, E., Marchetti, S., and Nova, R., Design Parameters for Soft Clays: General Report, *In Proceedings of the 7th European Conference on Soil Mechanics and Foundation Engineering*, Brighton, England, 5, 1979, pp. 27–57.
17. Coduto, D.P., *Foundation Design: Principles and Practices, Second Edition*, Prentice-Hall, New Jersey, 2001.
18. Look, B.G., *Handbook of Geotechnical Investigation and Design Tables*, Taylor & Francis, London, 2007.
19. Das, B.M., *Advanced Soil Mechanics, Third Edition,* Taylor & Francis, New York, 2008.
20. Das, B.M., *Principles of Foundation Engineering, Eighth Edition*, Cengage Learning, Boston, 2014.
21. Meyerhof, G.G. Bearing Capacity and Settlement of Pile Foundations, *Journal of Geotechnical and Environmental Engineering*, ASCE, 102(GT3), 1976, pp. 197-228.
22. Tomlinson, M. and Woodward, J., *Pile Design and Construction Practice, Fifth edition*, Taylor & Francis, London, 2008.
23. Lim, A., Batistuta, V.H., and Wijaya, Y.V.C., Finite Element Modelling of Prestressed Concrete Piles inf Soft Soils, Case Study: Northern Jakarta, Indonesia, *Journal of the Civil Engineering Forum*, 8(1), 2023, 21-30. https://doi.org/10.22146/jcef.3597
24. Saptyanto, K., *Hitung Balik Nilai Kekakuan Tanah dari Hasil Pile Loading Test dengan Menggunakan Program Plaxis, Skripsi*, Universitas Bina Nusantara, 2012.
25. Rahardjo, P.P., Manual Pondasi Tiang, Edisi ke-5, Geotechnical Engineering Center, Bandung, 2017.
26. Liao, S.S.C. and Whitman, R.V., Overburden Correction Factors for SPT in Sand, *Journal of Geotechnical Engineering*, 112(3), 1986, pp. 373–377. https://doi.org/10.1061/(ASCE)0733-9410(1986)112:3(373)